

Is an Electronic Shield at the Molecular Origin of Lead Poisoning? A Computational Modeling Experiment**

Christophe Gourlaouen and Olivier Parisel*

As a very malleable metal characterized by a very low melting point, lead has been used, pure or as salts, since the Bronze Age.^[1] Nowadays, the global production of lead is still increasing and amounts to several billion tons per year, essentially devoted to batteries, glasses, ceramics, or electronics.

Lead has become the pollutant metal that is the most widely scattered in the world,^[2] its toxic effects and disastrous influences on public health have been known since antiquity.^[3,4] This pollution became explosive in the Industrial Revolution. In the 1920s, it was (re)discovered that Pb(Et)₄ had powerful antidetonant properties when admixed with gasoline. This has resulted in a large-scale global dissemination^[5] as attested to by Greenland's ices.^[1,6]

The massive use of lead in industry, together with the variety and the seriousness of its effects on human health, especially that of children,^[7–9] have justified investigating the relationships between lead exposure and a large number of clinical symptoms (lead poisoning or saturnism). However, few works have been devoted to how lead poisoning acts at the molecular level. It is, however, known that lead, and its derivatives, target many parts of the human organism^[10] as they follow the biochannels devoted to calcium, zinc, magnesium, or iron.^[11,12] The current detoxication therapies rely on chelators such as ethylenediaminetetraacetate, 2,3-dimercaptopropanol, *meso*-2,3-dimercaptosuccinic acid, or penicillamine.^[13] These agents suffer, however, the drawback of lacking selectivity towards Pb²⁺. Moreover, side effects such as redeposition from a targeted organ to another are known to occur.^[14] In line with our previous investigations on Pb²⁺ compounds,^[15] we herein use quantum chemistry (density functional theory (DFT) computations that rely on relativistic pseudopotentials to account for the relativistic effects lead is subject to) to track the structural changes induced upon exchanging native Ca^{II} or Zn^{II} cations for Pb²⁺ cations in models of two well-known targeted proteins: calmodulin and δ -aminolevulinic acid dehydratase (ALAD). Ca²⁺, Zn²⁺, and Pb²⁺ ions have different ionic radii $r(M)$ ($M =$

metal, Table 1 and Table 2)^[16] and electronic configurations: [Ar]4s⁰, [Ar]3d¹⁰4s⁰, and [Xe]4f¹⁴5d¹⁰6s²6p⁰, respectively. Pb^{II} complexes thus exhibit a metallic lone pair with either a holo- or a hemidirected character (Figure 1).^[17]

Calmodulin is a Ca^{II}-binding protein involved in processes such as cell mitosis and growth, neurotransmission, and regulation of the calcium pump.^[18] It is subject to Pb²⁺ substitution.^[19–21] It has four identical sites to which four Ca²⁺ cations bind sequentially (PDB code: 1CLL).^[22,23] They

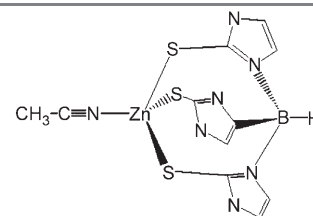
Table 1: Structural parameters (bond lengths [Å]; valence angles [°]) for the model of calmodulin before and after substitution by a Pb²⁺ cation.^[a]

Parameter	M = Ca ²⁺	M = Pb ²⁺
$r(M)$	0.99	1.19
M–O ¹	2.51	2.64
M–O ²	2.59	2.38
M–O ³	2.49	2.69
M–O ⁴	2.47	3.06
M–O ⁵	2.51	3.13
M–O ⁶	2.38	2.49
M–O ⁷	2.48	2.78
O ¹ –M–O ⁷	165.9	149.5
O ⁶ –M–O ²	85.4	81.7
O ² –M–O ³	51.7	51.5
O ³ –M–O ⁴	79.9	68.0
O ⁴ –M–O ⁵	82.7	68.0
O ⁵ –M–O ⁶	91.5	85.9
O ⁶ –M–C ¹	95.7	107.6
C ¹ –M–O ⁴	90.9	89.8
Ω [°]	360.8	351.3
$V(Pb)$ [Å ³]	17.2	23.4

[a] An ideal pentagonal-bipyramidal structure would have an axial angle for O₁–M–O₇, amounting to 180.0° and a sum over the equatorial valence angles ($\Omega = O_6$ –M–C₁ + C₁–M–O₄ + O₄–M–O₅ + O₅–M–O₆) amounting to 360°. See reference [32] for details concerning $V(Pb)$.

Table 2: Structural parameters for the model of δ -ALAD before and after substitution by a Pb²⁺ cation.^[a]

	M = Zn ²⁺	M = Pb ²⁺
$r(M)$	0.74	1.19
$d(M-S)$	2.35	2.79
$d(M-B)$	3.59	4.31
$d(M-N)$	2.09	3.35
$\Theta(S-M-S)$	109.2°	90.6°
$\Omega(M-S_3)$	327.6°	271.8°
$V(Pb)$ [Å ³]	20.1	34.4



[a] Θ is the average of the (S–M–S) valence angles. Ω is the sum of these three angles: a value of 360° would indicate local planarity (D_{3h}). Distances are in Å. See reference [32] for details concerning $V(Pb)$.

[*] Dr.-Ing. C. Gourlaouen, Dr. O. Parisel
Laboratoire de Chimie Théorique – UMR 7616 CNRS/UPMC
Université Pierre et Marie Curie – Paris 6
Case Courrier 137-4, place Jussieu
75252 Paris CEDEX 05 (France)
Fax: (+33) 1-4427-4117
E-mail: parisel@lct.jussieu.fr
Homepage: <http://www.lct.jussieu.fr>

[**] This research was supported by the French IDRIS (Orsay) and CINES (Montpellier) national supercomputing centers. The authors are indebted to Dr. H. Gérard (LCT, Paris VI) and Dr. J. Maddaluno (IRCOF, Rouen) for stimulating discussions.

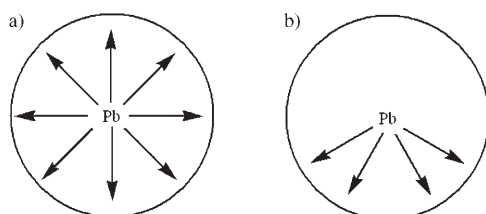


Figure 1. The two structural families of Pb^{II} complexes: a) holodirected and b) hemidirected.^[17]

have been modeled by means of a heptacoordinated Ca^{2+} cation, binding one acetate residue, three acetic groups, one water molecule, and one amide function from the backbone. The resulting geometry is close to a holodirected pentagonal bipyramid (Figure 2, left). The substitution of Ca^{II} by Pb^{2+} induces structural distortions (Figure 2, right), but the coordination number at the cation does not change. The spatial

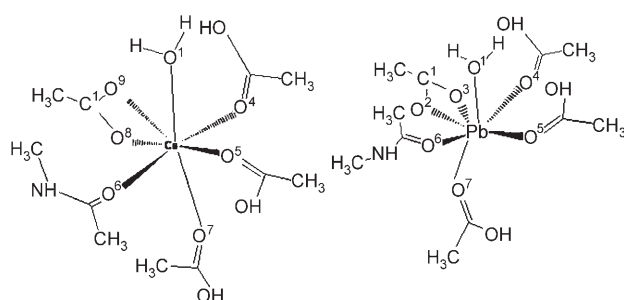


Figure 2. Bioinspired models of metallated sites of calmodulin (left: native Ca^{II} ; right: Pb^{2+} substituted). The systems carry one positive net charge.

expansion of the site clearly increases. In the Ca^{II} complex, all $\text{Ca}-\text{O}$ bond lengths are between 2.4 Å and 2.5 Å (Table 1), but between 2.3 Å and 3.2 Å in the Pb^{II} complex. One acetic acid ($\text{Pb}-\text{O}^4$: 3.06 Å) and one acetate ($\text{Pb}-\text{O}^5$: 3.13 Å) barely bind to the metal cation. The substitution does not imply any departure from an ideal equatorial plane: Ω decreases by only 9.5° (Table 1). The axial $\text{O}^1-\text{M}-\text{O}^7$ angle is reduced in the Pb^{II} complex. This is owing to the emergence of the $6s^2$ lone pair, which induces a slightly hemidirected character (Figure 3, top). The electron localization function (ELF) analysis reveals that $V(\text{Pb})$ increases from 17.2 to 23.4 Å³ upon relaxation and is populated by 2.41 electrons, indicating a moderate charge transfer of 0.41 from the ligands to the 6p shell of the cation.

The conservation of the general shape upon substitution, together with that of the coordination number at the cation, might explain why Pb^{2+} activates calmodulin as Ca^{2+} does: both Ca^{2+} and Pb^{2+} can accommodate high coordination numbers, which can be achieved for only very few structural arrangements. This result is in line with the experimental fact that neither a complete reorganization of the protein nor a full inhibition of the biochemical activity has been observed for calmodulin upon substitution by Pb^{2+} .

δ -ALAD, a Zn^{II} protein also called porphobilinogen synthase,^[24] plays a fundamental role in heme biosynthesis: it

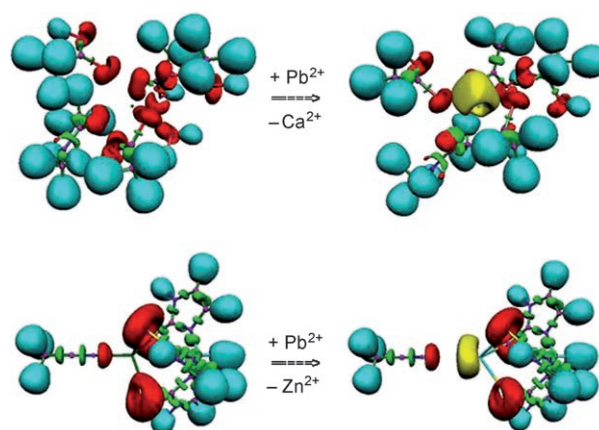


Figure 3. ELF function localization domains ($\eta=0.85$). The $V(\text{X},\text{H})$ basins are shown in turquoise, the lone pair basins in red, the core basins in magenta, and the disynaptic valence basins in green. The $6s$ shell, essentially the $6s^2$ lone pair, is represented by the large shaded yellow $V(\text{Pb})$ basin. Top: bioinspired calmodulin model for the Ca^{II} (left) and Pb^{II} (right) complexes. Bottom: bioinspired ALAD model for the Zn^{II} (left) and Pb^{II} (right) complexes.

converts two molecules of δ -aminolevulinic acid (ALA) into porphobilinogen. Inhibiting δ -ALAD one way or another thus induces anemia. It also induces, consequently, the accumulation of ALA, which is a neurotoxin. δ -ALAD is one of the most deeply investigated lead targets by physical chemistry.^[12,25–27] The structure of the Zn^{II} native site is tetrahedral (PDB code: 1E51),^[22,28] a commonly encountered coordination for Zn^{2+} , but exhibits an atypical Cys_3 environment.^[29] ALAD has been the subject of bioinspired modeling by a tris(2-mercapto-1-phenylimidazolyl)hydroborato ligand (Tm^{Ph}):^[30,31] the $[(\text{Tm}^{\text{Ph}})\text{Zn}]^+$ complex is very similar^[11] to the native site and mimics its structural rigidity. In the simplified model used here (see structure in Table 2), the phenyl moieties have been replaced by hydrogen atoms; the Zn^{2+} ion binds three sulfur atoms from three S-deprotonated 2-mercapto-imidazole moieties that mimic those of cysteine residues. Bridging the imidazole moieties by a boron atom ensures the formation of a cage structure. Acetonitrile mimics the native substrate.

Substitution by the Pb^{2+} cation induces strong distortions (Table 2). The $\text{Pb}-\text{S}$ bond lengths (2.79 Å), although quite short, are increased by about 0.4 Å with respect to the initial $\text{Zn}-\text{S}$ bond lengths. This value compares fairly well with that reported for a number of PbS_3 models (2.64 Å) and with that reported for $[(\text{Tm}^{\text{Ph}})\text{Pb}][\text{ClO}_4]$ (2.67 or 2.69 Å),^[28,30] $[(\text{Tm}^{\text{Ph}})\text{Pb}]^+$ (2.7 Å), or $\text{Pb}^{\text{II}}-\text{ALAD}$ (2.8 Å).^[25,30] The torsion of the cycles (the $\text{Pb}-\text{S}-\text{N}-\text{B}$ dihedral angle) increases by about 14°, and the $\text{M}-\text{B}$ distance increases by about 0.7 Å upon substitution. The mean $\text{S}-\text{M}-\text{S}$ valence angle (Θ , Table 2) decreases by about 20° and Ω , the sum of the $\text{S}-\text{M}-\text{S}$ angles, plummets by more than 50°: the substitution thus enhances the trigonal-pyramidal character at the metal cation. Simultaneously, the cation–acetonitrile bond breaks: the $\text{Pb}-\text{N}$ bond length increases to 3.35 Å, much larger than the sum of the covalent radii of the two atoms (2.17 Å), whereas in the Zn^{II} complex, it amounts to 2.01 Å. Although this complex is

tetracoordinated, tetrahedral, and holodirected, the Pb^{II} analogue clearly appears tricoordinated, hemidirected, and trigonal pyramidal.

This change is related to the localization of the lone pair of the Pb^{2+} cation as clearly seen by the ELF analysis (Figure 3, bottom). Before substitution, the lone pair of the acetonitrile ligand points towards the acceptor Zn^{2+} cation, whereas afterwards, it faces that of the Pb^{2+} cation. A competition is thus triggered between the repulsion of these two lone pairs and the electrostatic attraction between the polar acetonitrile and the cationic charge. Here, the second effect is not efficient enough as the fourth ligand no longer binds. The ELF analysis also shows that $V(\text{Pb})$ is populated by 2.85 electrons. Its volume has increased from 20.1 to 34.4 Å³. This latter value is significantly larger than that observed for calmodulin: a strong directionality of the lone pair has appeared.

Such drastic changes could explain why the Pb^{2+} cation inactivates δ -ALAD. Upon substitution, the thiophilicity of the Pb^{2+} cation acts as the driving force: the less donating ligand, acetonitrile, which is a model of the native substrate, is expelled from the first coordination sphere of the metal cation for the Pb^{2+} lone pair to become hemidirected. Upon substitution, $V(\text{N})$ of the acetonitrile ligand increases from 37.7 to 44.3 Å³. As anticipated from ALAD mutants^[24] and deduced from X-ray measurements,^[31] the Pb^{2+} cation tends to avoid four coordination: it remains tricoordinated (Figure 3) and its lone pair acts as a strong electronic shield repelling the extra nucleophilic ligand.

In conclusion, based on scalar relativistic pseudopotential DFT calculations and analyses performed on two models of proteins targeted by lead, the substitution of Zn^{II} and Ca^{II} by the Pb^{2+} cation has been investigated. In the case of ALAD, the substitution induces a drastic reorganization at the metal center: the model of the native substrate is expelled and strong structural distortions are observed. From the topological point of view, the initial holodirected, tetrahedral, tetracoordinated site evolves into a tricoordinated, hemidirected, trigonal site. Such a dramatic effect is expected to disrupt the natural function of the metallated domain, which could induce a complete inhibition. In the case of calmodulin, things are more subtle. Although some distortions appear upon the substitution, less pronounced changes than in ALAD occur. The native holodirected structure becomes rather hemidirected. The resulting perturbation on the protein may not be strong enough to fully inhibit its biochemical activity. Additional computations performed on a set of model structures^[33] support the previous conclusions: sulfur-rich Zn^{II} sites behave roughly as ALAD and are dramatically affected by the Pb^{2+} cation, whereas Ca^{II} sites behave as calmodulin. It is therefore expected that the solution to saturnism may not rely on a single compound as a distinction should be made between Zn^{II} - and Ca^{II} -native proteins. Surprisingly, the fact that Pb^{II} complexes can be classified as hemi- or holodirected according to the directional or nondirectional character of the 6s² lone pair seems to have always been considered as anecdotic even though it could indeed be a key feature to design future Pb^{2+} -sequestering ligands. From the clear-cut insight obtained above, one can expect that novel, efficient agents should

exhibit appendages: 1) putting the Pb^{2+} cation in a tricoordinated sulfur-rich environment to ensure thiophilicity, and 2) stabilizing the 6s² lone pair, the expansion of which seems to be the driving force for the structural distortions encountered. From this point of view, improvable precursors could be endogenous chelators^[34] or decorporating substances encountered in phytochelation processes.^[35]

Computational Section

Computations: All calculations were performed by using the Gaussian03 package^[36] within the DFT framework (B3LYP). The standard 6-31 + G** basis sets were used for B, C, H, O, S, and N atoms. In previous work, we have compared the performance of using all-electron (AE) relativistic four-component calculations or scalar relativistic pseudopotentials calculations,^[15] and we have retained the SDD pseudopotentials,^[37] coupled to double-zeta basis sets obtained from the (4s,4p,1d)/[2s,2p,1d] (Pb^{2+}), (4s,4p)/[2s,2p] (Ca^{2+}), and (4s,2p)/[3s,2p] (Zn^{2+}) contractions.

Analysis: The electronic densities were investigated by means of the topological analysis of the ELF function^[38,39] by using the TopMod package.^[40,41] Within this framework, space is partitioned into basins of attractors, each of them having a chemically relevant meaning. These basins are classified as: 1) core basins $C(X)$ surrounding nuclei X , which are usually representative of electrons not involved in the chemical bonding (nonvalence and internal-shell electrons) and 2) valence basins, which are characterized by their synaptic order, namely the number of core basins with which they share a common boundary. The valence basin $V(X)$ is monosynaptic and corresponds to lone-pair or nonbonding regions. The $V(X,Y)$ basin is disynaptic: it binds the core basins of two nuclei X and Y and, thus, corresponds to a bonding region between X and Y .

Received: July 27, 2006

Revised: November 9, 2006

Published online: December 7, 2006

Keywords: calmodulin · density functional calculations · ELF (electron localization function) · proteins · saturnism

- [1] K. J. R. Rosman, W. Chisholm, S. Hong, J.-P. Candelone, C. F. Boutron, *Environ. Sci. Technol.* **1997**, *31*, 3413; I. Renberg, R. Bindler, M.-L. Brännvall, *Holocene* **2001**, *11*, 511.
- [2] C. C. Patterson, *Arch. Environ. Health* **1965**, *11*, 344.
- [3] H. A. Waldron, *Lancet* **1973**, *302*, 626; T. Waldron, *Lancet* **1978**, *312*, 1315; J. Scarborough, *J. Hist. Med.* **1984**, *39*, 469; S. C. Gilfillan, *J. Occup. Med.* **1965**, *7*, 53; L. Needleman, D. Needleman, *Class. Views* **1985**, *4*, 63.
- [4] S. Hernberg, *Am. J. Ind. Med.* **2000**, *38*, 244; J. Eisinger, *Med. Hist.* **1982**, *26*, 279; H. A. Waldron, *Med. Hist.* **1973**, *17*, 391.
- [5] H. L. Needleman, *Environ. Res.* **2000**, *84*, 20; H. L. Needleman, *Environ. Res.* **1998**, *78*, 79; H. L. Needleman, *Environ. Res.* **1997**, *74*, 95.
- [6] J. R. McConnell, G. W. Lamorey, M. A. Hutterli, *Geophys. Res. Lett.* **2002**, *29*, 2130; K. J. R. Rosman, W. Chilsom, J. P. Candelone, S. Hong, C. F. Boutron, *Geochim. Cosmochim. Acta* **1994**, *58*, 3265.
- [7] "Lead Neurotoxicity": D. A. Cory-Slechta, J. G. Pound in *Handbook of Neurotoxicology* (Eds.: L. W. Chang, R. S. Dyers), Marcel Dekker, New York, **1995**.
- [8] Y. Finkelstein, M. E. Markowitz, J. F. Rosen, *Brain Res. Rev.* **1998**, *27*, 168; D. E. Glotzer, H. Bauchner, *Pediatrics* **1992**, *89*, 614.

- [9] For recent statistics concerning China, see: S. Wang, J. Zhang, *Environ. Res.* **2006**, *101*, 412.
- [10] B. P. Lanphear, R. Hornung, J. Khoury, K. Yolton, P. Baghurst, D. C. Bellinger, R. L. Canfield, K. N. Dietrich, R. Bornsheim, T. Greene, S. J. Rothenberg, H. L. Needleman, L. Schnaas, G. Wasserman, J. Graziani, R. Roberts, *Environ. Health Perspect.* **2005**, *113*, 894; B. B. Gump, P. Stewart, J. Reihman, E. Lonky, T. Darvill, K. A. Matthews, P. J. Parsons, *Neurotoxicol. Teratol.* **2005**, *27*, 655; K. D. Rosenman, A. Sims, Z. Luo, J. Gardiner, *J. Occup. Environ. Med.* **2003**, *45*, 546; S. Araki, H. Sato, K. Yokoyama, K. Murata, *Am. J. Ind. Med.* **2000**, *37*, 193.
- [11] J. C. Payne, M. A. ter Horst, H. A. Godwin, *J. Am. Chem. Soc.* **1999**, *121*, 6850.
- [12] H. A. Godwin, *Curr. Opin. Chem. Biol.* **2001**, *5*, 223.
- [13] O. Andersen, *Chem. Rev.* **1999**, *99*, 2683; E. L. Liebelt, M. W. Shannon, *Pediatr. Ann.* **1994**, *23*, 616.
- [14] S. J. S. Flora, G. M. Kannan, B. P. Pant, *Arch. Toxicol.* **2002**, *76*, 269; S. J. S. Flora, R. Bhattacharya, R. Vijayaraghavan, *Fundam. Appl. Toxicol.* **1995**, *25*, 233; W. Zheng, R. M. Maiorino, K. Brendel, H. V. Aposhian, *Fundam. Appl. Toxicol.* **1990**, *14*, 598.
- [15] C. Gourlaouen, J.-P. Piquemal, T. Saue, O. Parisel, *J. Comput. Chem.* **2006**, *27*, 142; C. Gourlaouen, J.-P. Piquemal, O. Parisel, *J. Chem. Phys.* **2006**, *124*, 174311; C. Gourlaouen, H. Gérard, O. Parisel, *Chem. Eur. J.* **2006**, *12*, 5024.
- [16] J. E. Huheey, E. A. Keiter, R. L. Keiter, *Inorganic Chemistry: Principles of Structure and Reactivity*, Harper & Collins, New York, **1993**.
- [17] L. Shimoni-Livny, J. P. Glusker, C. W. Bock, *Inorg. Chem.* **1998**, *37*, 1853.
- [18] D. Chin, A. R. Means, *Trends Cell Biol.* **2000**, *10*, 322; D. Campagna, G. Huel, G. Hellier, F. Girard, J. Sahuquillo, A. Fagot-Campagna, J. Godin, P. Blot, *Life Sci.* **2000**, *68*, 203.
- [19] C. M. L. S. Bouton, L. P. Frelin, C. E. Forde, H. A. Godwin, J. Pevsner, *J. Neurochem.* **2001**, *76*, 1724.
- [20] G. Goldstein, *Neurotoxicology* **1993**, *14*, 97; C. S. Fullmer, S. Edelstein, R. H. Wasserman, *J. Biol. Chem.* **1985**, *260*, 6816; S. H. Chao, Y. Suzuki, J. R. Zysk, W. Y. Cheung, *Mol. Pharm.* **1984**, *26*, 75; E. Habermann, K. Crowell, P. Janicki, *Arch. Toxicol.* **1983**, *54*, 61; H. Ouyang, H. J. Vogel, *Biometals* **1998**, *11*, 213; C. Ferguson, M. Kern, G. Audesirk, *Neurotoxicology* **2000**, *21*, 365; R. H. S. Westerink, A. A. Klompmakers, H. G. M. Westenberg, H. P. M. Vijverberg, *Brain Res.* **2002**, *957*, 25.
- [21] M. A. Wilson, A. T. Brunger, *Acta Crystallogr. Sect. D* **2003**, *59*, 1782.
- [22] <http://www.pdb.org>
- [23] R. Chattopadhyaya, W. E. Meador, A. R. Means, F. A. Quirocho, *J. Mol. Biol.* **1992**, *228*, 1177.
- [24] E. K. Jaffe, J. Martins, J. Li, J. Kerniven, R. L. Dunbrack, Jr., *J. Biol. Chem.* **2001**, *276*, 1531.
- [25] T. J. B. Simons, *Eur. J. Biochem.* **1995**, *234*, 178; M. J. Warren, J. B. Cooper, S. P. Wood, P. M. Shoolingin-Jordan, *Trends Biochem. Sci.* **1998**, *23*, 217.
- [26] J. C. Payne, B. W. Rous, A. L. Tenderholt, H. A. Godwin, *Biochemistry* **2003**, *42*, 14214.
- [27] A. B. Ghering, L. M. Miller Jenkins, B. L. Schenck, S. Deo, R. A. Mayer, M. J. Pikaart, J. G. Omichinski, H. A. Godwin, *J. Am. Chem. Soc.* **2005**, *127*, 3751.
- [28] N. L. Mills-Davies, PhD thesis, University of Southampton, UK, **2001**; P. T. Erskine, L. Coates, R. Newbold, A. A. Brindley, F. Stauffer, G. D. E. Beaven, R. Gill, A. Cocker, S. P. Wood, M. J. Warren, P. M. Shoolingin-Jordan, R. Neier, J. B. Cooper, *Acta Crystallogr. Sect. D* **2005**, *61*, 1222.
- [29] L. Coates, G. Beaven, P. T. Erskine, S. I. Beale, S. P. Wood, P. M. Shoolingin-Jordan, J. B. Cooper, *Acta Crystallogr. Sect. D* **2005**, *61*, 1594; T. Simonson, N. Calimet, *Proteins Struct. Funct. Genet.* **2002**, *49*, 37.
- [30] B. M. Bridgewater, G. Parkin, *J. Am. Chem. Soc.* **2000**, *122*, 7140; G. Parkin, *Chem. Rev.* **2004**, *104*, 699.
- [31] J. S. Magyar, T.-C. Weng, C. M. Stern, D. F. Dye, B. W. Rous, J. C. Payne, B. M. Bridgewater, A. Mijovilovich, G. Parkin, J. M. Zalwski, J. E. Penner-Hahn, H. A. Godwin, *J. Am. Chem. Soc.* **2005**, *127*, 9495.
- [32] V(Pb) represents the volume of the valence monosynaptic basin of the Pb²⁺ cation, which, chemically, corresponds to the *n* = 6 shell. For the native structures, it is computed by putting the Pb²⁺ cation in place of the native cations before any structural reorganization.
- [33] C. Gourlaouen, PhD Thesis, University Paris VI, France, **2006**.
- [34] C. Huo, C. Wang, M. Zhao, S. Peng, *Chem. Res. Toxicol.* **2004**, *12*, 1112.
- [35] D. L. Callahan, A. J. M. Baker, S. D. Kolev, A. G. Weed, *J. Biol. Inorg. Chem.* **2006**, *11*, 2; M. Ghosh, S. P. Singh, *Appl. Ecol. Environ. Res.* **2005**, *3*, 1; C. S. Cobbett, *Plant Physiol.* **2000**, *123*, 825; S. A. Hamidinia, B. Tan, W. L. Erdahl, C. J. Chapman, R. W. Taylor, D. R. Pfeiffer, *Biochemistry* **2004**, *43*, 15956; G. Scarano, E. Morelli, *Biometals* **2002**, *15*, 145; P. Sharma, R. S. Dubey, *Braz. J. Plant Physiol.* **2005**, *17*, 35;
- [36] Gaussian03, Revision C.02, M. J. Frisch, G. W. Trucks, H. B. Schlegel, G. E. Scuseria, M. A. Robb, J. R. Cheeseman, J. A. Montgomery, Jr., T. Vreven, K. N. Kudin, J. C. Burant, J. M. Millam, S. S. Iyengar, J. Tomasi, V. Barone, B. Mennucci, M. Cossi, G. Scalmani, N. Rega, G. A. Petersson, H. Nakatsuji, M. Hada, M. Ehara, K. Toyota, R. Fukuda, J. Hasegawa, M. Ishida, T. Nakajima, Y. Honda, O. Kitao, H. Nakai, M. Klene, X. Li, J. E. Knox, H. P. Hratchian, J. B. Cross, V. Bakken, C. Adamo, J. Jaramillo, R. Gomperts, R. E. Stratmann, O. Yazyev, A. J. Austin, R. Cammi, C. Pomelli, J. W. Ochterski, P. Y. Ayala, K. Morokuma, G. A. Voth, P. Salvador, J. J. Dannenberg, V. G. Zakrzewski, S. Dapprich, A. D. Daniels, M. C. Strain, O. Farkas, D. K. Malick, A. D. Rabuck, K. Raghavachari, J. B. Foresman, J. V. Ortiz, Q. Cui, A. G. Baboul, S. Clifford, J. Cioslowski, B. B. Stefanov, G. Liu, A. Liashenko, P. Piskorz, I. Komaromi, R. L. Martin, D. J. Fox, T. Keith, M. A. Al-Laham, C. Y. Peng, A. Nanayakkara, M. Challacombe, P. M. W. Gill, B. Johnson, W. Chen, M. W. Wong, C. Gonzalez, J. A. Pople, Gaussian Inc., Wallingford CT, **2004**.
- [37] D. Andrae, U. Haeussermann, M. Dolg, H. Stoll, H. Preuss, *Theor. Chim. Acta* **1990**, *77*, 123.
- [38] A. D. Becke, K. E. Edgecombe, *J. Chem. Phys.* **1990**, *92*, 5397; A. Savin, R. Nesper, S. Wengert, T. F. Fässler, *Angew. Chem.* **1997**, *109*, 1892; *Angew. Chem. Int. Ed. Engl.* **1997**, *36*, 1808; B. Silvi, A. Savin, *Nature* **1994**, *371*, 683; A. Savin, B. Silvi, F. Colonna, *Can. J. Chem.* **1996**, *74*, 1088.
- [39] For a recent review, see: J. Poater, M. Duran, M. Solà, B. Silvi, *Chem. Rev.* **2005**, *105*, 3911; E. Matito, B. Silvi, M. Duran, M. Solà, *J. Chem. Phys.* **2006**, *125*, 024301.
- [40] S. Noury, X. Krokidis, F. Fuster, B. Silvi, TopMod Package, **1997**. This package is available on the web site of the Laboratoire de Chimie Théorique, Université Pierre et Marie Curie (UMR CNRS/UPMC 7616), URL: <http://www.lct.jussieu.fr>.
- [41] S. Noury, X. Krokidis, F. Fuster, B. Silvi, *Comput. Chem.* **1999**, *23*, 597.